Osteoarthritis and Cartilage 23 (2015) 1186–1193

Osteoarthritis and Cartilage

Meniscal biomechanical alterations in an ACLT rabbit model of early osteoarthritis

A. Levillain †, C. Boulocher ‡, S. Kaderli §, E. Viguier ‡, D. Hannouche ||, T. Hoc † *, H. Magoariec †

† LTDS, UMR CNRS 5513, Université de Lyon, Ecole centrale de Lyon, 36 av Guy de Collongue, 69134 Ecully Cedex, France
‡ Research Unit ICE, UPSP 2011.03.101, Université de Lyon, Veterinary Campus of VetAgro Sup, 69 280 Marcy l'Etoile, France
§ School of Pharmaceutical Sciences, University of Geneva and Lausanne, Quai Ernest-Ansermet 30, 1211 Geneva, Switzerland
|| B2OA, UMR CNRS 7052 CHU Lariboisière Saint Louis, 10 av de Verdun, 75020 Paris France

ARTICLE INFO

Article history:
Received 12 December 2014
Accepted 18 February 2015

Keywords:
Meniscus
Osteoarthritis
Indentation
Collagen
Glycosaminoglycan

SUMMARY

Objective: The purpose of this study was to analyze the early biomechanical alterations of menisci during the early stage of osteoarthritis (OA) development and to correlate them with the chemical composition and matrix alteration. A particular focus was paid to pathological changes in glycosaminoglycan (GAG) content and collagen fiber architecture.
Design: Menisci ($n = 24$) were removed from rabbits' knee joints 6 weeks following surgical anterior cruciate ligament transection (ACLT). Both the anterior and posterior regions of medial and lateral menisci were characterized using indentation tests, Raman microspectroscopy (RM), biphotonic confocal microscopy (BCM) and histology.
Results: Mechanical and matrix alterations occurred in both regions of medial and lateral menisci. A significant decrease in the mechanical properties was observed in OA menisci, with a mean reduced modulus from 2.3 to 1.1 MPa. Microstructural observations revealed less organized and less compact collagen bundles in operated menisci than in contralateral menisci, as well as a loss of fiber tension. GAG content was increased in OA menisci, especially in the damaged areas. Neither changes in the secondary structure of collagen nor mineralization were detected through RM at this stage of OA.
Conclusion: ACLT led to a disorganization of the collagen framework at the early stage of OA development, which decreases the mechanical resistance of the menisci. GAG content increases in response to this degradation. All of these results demonstrate the strong correlation between matrix and mechanical alterations.

Introduction

Menisci play a fundamental role in the load distribution within the knee. They transmit more than 50% of the total load applied in the human joint and ensure its congruence[1]. When these functions are not fulfilled efficiently, particularly due to meniscus degradation, the contact stresses in the meniscal compartments increase[2], leading to cartilage loss and subchondral bone defects[2,3]. These alterations contribute to the progression of osteoarthritis (OA). To prevent this occurrence, knowledge of how menisci are damaged is necessary.

Meniscal lesions are very common in human knees in advanced-stage OA. Their pattern and regional variation have been extensively studied macroscopically or through magnetic resonance imaging[4–6]. Over the past decade, further investigations have been conducted into the chemical, microstructural and mechanical alterations of human menisci. They revealed alteration of the mechanical properties[7,8], disorganization of the collagen network[8–10], formation of calcifications[10,11] and controversial changes in glycosaminoglycan (GAG) and collagen contents[7,9,10]. However, in these studies, the severity of OA damage makes it difficult to determine the chronology of the different components' degradation and their relation to the mechanical impairment. It is thus

* Address correspondence and reprint requests to: Hoc T., LTDS, UMR CNRS 5513, Université de Lyon, Ecole centrale de Lyon, 36 av Guy de Collongue, 69134 Ecully Cedex, France.
E-mail address: thierry.hoc@ec-lyon.fr (T. Hoc).

http://dx.doi.org/10.1016/j.joca.2015.02.022
1063-4584/

necessary to analyze the tissue at an early stage of OA, using animal models.

Anterior, i.e., cranial, cruciate ligament transection (ACLT) in rabbits is among the most suitable models of early OA in humans[12]. It has been widely used to evaluate early structural changes in cartilage[13,14], but to date, only a few studies have focused on the meniscus[15,16]. Recently, one study focused on the mechanical properties and GAG content of rabbit menisci in a mixed model, using both ACL and menisci transections[17]. A decrease in the compressive moduli and GAG content were found after 12 weeks. However, Hellio Le Graverand *et al.*[16] found inconsistent results when the menisci were left intact during the ACLT procedure. GAG content increased during the early stage following ACLT, at 3 and 8 weeks. A loss of orientation of the collagen fibers, which are also involved in the mechanical resistance of the menisci[18], occurred as well. The role of GAGs and collagen fibers in the compression properties of the menisci is extremely controversial in the literature[7,17,19,20]. Hence, the effect of these complex alterations on the mechanical properties of the menisci is still unknown.

The aim of this study was to analyze the early changes in the mechanical properties of OA rabbit menisci following ACLT and to correlate them with matrix alterations. Attention was paid to variations between the frequently affected posterior region[10] and the anterior region. The mechanical properties, chemical composition, collagen fiber organization and GAG content were assessed through microindentation, Raman microspectroscopy (RM), biphotonic confocal microscopy (BCM) and histology, respectively.

Material and method

Animal model

The experimental work on animals was performed in the experimental medicine and surgery center of the Claude Bourgelat Institute, under the authorization of the ethical committee of VetAgro Sup (Lyon, authorization number 1373) and in full accordance with European legislation. Six healthy adult (5 months of age, 3.7 kg on average) male New Zealand white rabbits provided by Centre Lago (Vonnas, France) were used. After 2 weeks in acclimation and quarantine, experimental OA was surgically induced in the left knee by ACLT, by a trained veterinary surgeon.

Before surgery, the animals received subcutaneous injections of Borgal® (sulfadoxine and trimethoprim) 30 mg/kg twice, morphine 0.1 mg/kg, and Meloxidyl® (meloxicam) 0.4 mg/kg. Deep anesthesia was induced by intra-muscular (IM) injection of Ketamine 1000® 40 mg/kg and Domitor® (medetomidine) 80 µl/kg IM and then maintained by isoflurane 1–3.5% administered via endotracheal intubation. After careful shaving and disinfection (Vetedine® solution and soap), ACLT was performed on the left leg with a lateral approach[21], and the right knee was left intact. The complete rupture of the anterior cruciate ligament was assessed with the anterior drawer sign (manual horizontal dislocation) before the closure of the articular capsule. The operated leg was not immobilized, and rabbits were allowed to move freely in their individual cages after the surgery. For the purposes of this paper, the term “operated” will be used for the left ACLT knee and the term “contralateral” for the right non-operated knee. “Contralateral” term was preferred to “healthy” term as menisci can be affected due to possible weight transfer.

Postoperative care

The rabbits received buprenorphine 0.01 mg/kg SC for 4 days, Emeprid® (metoclopramide) 0.5 mg/kg SC for 3 days, Borgal® 15 mg/kg SC bid for 9 days and Feligastryl® 1cp/day for 3 days. Cothivet® spray was applied to the wound for 6 days after surgery. Veterinarians closely monitored recovery, and a careful clinical follow-up was performed every other day. These postoperative cares reduced pain and prevented the lameness. All rabbits fully recovered from the surgery. After a 6-week observation period[16,22,23], the rabbits were sacrificed by Dolethal® (pentobarbital) 1 ml/kg intra-vascular after being chemically restrained by IM injection of Ketamine 1000® 40 mg/kg and Domitor® 80 µg/kg. After a careful dissection of both knees, the menisci were detached from their attachments.

Experimental procedures

Immediately after removal, the menisci from three of the six rabbits were rinsed in Phosphate Buffered Solution (PBS) without calcium and magnesium and then fixed in 10% formalin for GAG quantification. Menisci were then embedded in paraffin and 4 µm-thick sections parallel to the tibial surface were sliced using a Microm HM 340 E microtome. In each sample, two representative slices (100 µm apart) were stained with Safranin O-fast green (SOFG), which turns GAG red, and hematoxylin/eosin (HE), which turns nuclei black and cytoplasm blue/green.

The menisci ($n = 12$) from the remaining three rabbits were stored at −20°C into wet compresses soaked into 10X PBS until they were utilized for subsequent biomechanical and micro-architectural analyzes. After thawing the menisci for 1 day in a refrigerator at 4°C, two slices measuring 2 mm wide were cut with a scalpel in anterior and posterior regions [Fig. 1(A)]. First, indentation tests in the circumferential direction, BCM, and RM were performed on the (x,z) plane, denoted radial plane [Fig. 1(B)]. Second, each sample was cut parallel to the tibial meniscal surface, approximately 1 mm from this surface. Indentation tests in the vertical direction and BCM were performed on the (x,y) plane, denoted tibial plane [Fig. 1(C)].

Indentation tests

Indentation tests were performed on meniscus samples immersed in 10X PBS, at ambient temperature, using a homemade device developed by Mattei *et al.*[24]. The indenter was a spherical polytetrafluoroethylene tip, with a radius of curvature, R, of 0.485 mm. The opposite face of indentation was glued onto a petri dish (glue 3, Loctite®). Along each direction, indentation tests were conducted on three locations in the center of the sample, composed of circumferential fibers[25], with a minimum spacing of 200 µm between two locations. Each test was repeated three times successively for each point and difference between reduced moduli was always less than 5%. To ensure reliability of the measurement, a reference material in Polymethyl methacrylate was indented before each series of tests on a given meniscus sample. For the loading path, a constant displacement rate of 2 µm s^{-1} and a maximum force of 1 mN were imposed to avoid surface and fibers disruption effects. The unloading path was carried out at the same displacement rate. For all indentation curves, the slope S at the initial point of the unloading part was determined and the reduced modulus E_r was calculated using Hertz theory[26] [Fig. 2, Eq. (1)]

$$E_r = \frac{\sqrt{\pi}}{2}\frac{S}{\sqrt{A}} = \frac{S}{2.\sqrt{\delta.R}}, \quad (1)$$

where A is the Hertz contact area and δ is the maximal penetration. We assumed that the beginning of penetration corresponded to a displacement at 0.05 mN force.

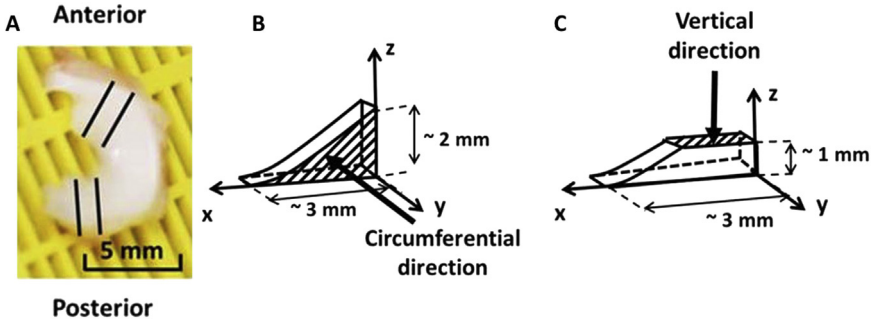

Fig. 1. Sample preparation procedure: A) optical image of a right lateral meniscus (contralateral) and localization of the two studied regions B) first cutting plane (the radial plane is hatched) and representation of the circumferential direction, C) second cutting plane (the tibial plane is hatched) and representation of the vertical direction.

In the present study, for each meniscus sample, only one value corresponding to the average of the nine moduli (three points with three measurements each) was considered.

Assessment of heterogeneity of the mechanical properties

The heterogeneity of the mechanical properties was assessed using three ratios.

The effect of meniscus microstructure, which predominantly consists of circumferential fibers, was assessed using the ratio between circumferential and vertical moduli E_r, denoted R_{ani} (ratio of anisotropy). For each knee, R_{ani} value averaged four ratios from measurements performed in Medial-Posterior, Medial-Anterior, Lateral-Posterior and Lateral-Anterior locations. According to this definition, $R_{ani} = 1$ would correspond to an isotropic behavior.

The effect of regional location was assessed using the ratio between posterior and anterior moduli E_r, denoted R_{reg}. For each knee, R_{reg} value averaged four ratios from measurements performed in Medial-Vertical, Medial-Circumferential, Lateral-Vertical and Lateral-Circumferential directions. According to this definition, $R_{reg} = 1$ would correspond to a homogeneous meniscus.

Finally, the effect of anatomical site was assessed using the ratio between lateral and medial moduli E_r, denoted R_{site}. For each knee, R_{site} value averaged four ratios from measurements performed in Posterior-Vertical, Posterior-Circumferential, Anterior-Vertical and Anterior-Circumferential directions. According to this definition, $R_{site} = 1$ would correspond to the same behavior for medial and lateral menisci.

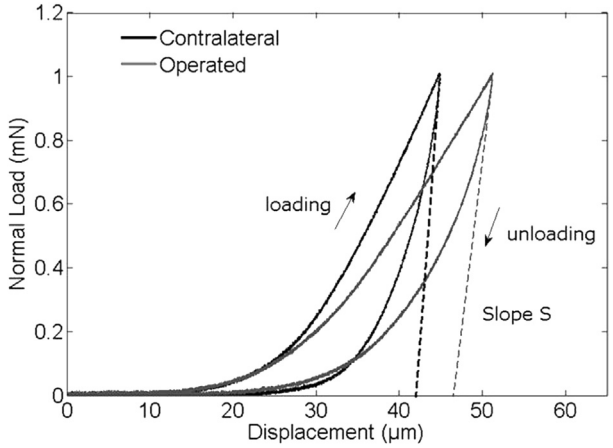

Fig. 2. Typical indentation curves of contralateral (black) and operated (grey) menisci. The dotted line represents the tangent (i.e., Slope S) to the curve at the initial point of the unloading part.

Chemical analyses

RM (LabRAM HR 800, Horiba Jobin Yvon, Villeneuve d'Ascq, France) was used in wet conditions on the radial plane. This technique uses Raman inelastic scattering to obtain information on the chemical composition of the material[27]. A 532-nm laser was used to excite the electrons within the material. The 40X immersion objective (LUMPLFLN 40XW, Olympus) and numerical aperture (NA) of 0.8 produced a laser spot approximately 0.8 μm in diameter. The acquisitions were made on the spectral range of 350 cm^{-1} – 1750 cm^{-1}, with an integration time of 30 s and one accumulation. Three spectra were acquired for each point, and six points were analyzed in all samples. The spectra were de-spiked, and the background was subtracted using a user-defined baseline correction routine in Matlab (The MathWorks Inc., Natick, Massachusetts, USA). Next, three spectra per point were averaged, and the resulting spectrum was smoothed using a sliding average over seven points algorithm in a Matlab routine. Finally, spectra were normalized to the phenylalanine ring breathing band intensity at 1004 cm^{-1}, which is distinct and constant between samples[28].

Microstructural observation

The collagen microstructure was observed through BCM (A1R MP PLUS®, Nikon), using an excitation wavelength of 850 nm. Second harmonic generated light from collagen and autofluorescent light from elastin were collected on two channels with specific band-pass filters of 400–490 and 500–550 nm, respectively. A 25X, 1.1 NA water immersion objective (CFI Apo LWD 25XW, Nikon) was used. The image field of view was 512 × 512 μm^2 with a resolution of 0.5 μm. For the radial plane, a mosaic image was built along *z*-axis in the sample center. For the tibial plane, three and two consecutive areas along the *x*-direction and *y*-direction, respectively, were imaged in the center of the sample. To scan the thickness of the meniscus, stacks of 2D images were recorded in each area, with a time scan of 2 s and an average of two scans per image, every 2 μm from 0 to 200 μm in depth. Finally, the whole stack of 2D images was projected using ImageJ 1.47v (NIH, Bethesda, Maryland, USA) on a single slice[29]. Each pixel of the output image contained the maximum value over all images in the stack at the particular pixel location. 3D reconstructions of image stacks of tibial plane acquisitions were performed using NIS-element Viewer (Nikon Instruments Europe B.V, France).

Detection of GAGs

Histological sections were imaged using an Eclipse TS100 microscope and a DS-FI2 color camera (Nikon instruments). The successive images were assembled using MosaicJ-ImageJ. Red

coverage of SOFG staining was semi-quantitatively analyzed using ImageJ[30]. Color images were first converted to Red-Green-Blue stacks and viewed as gray-scale images under green stack. Tissue appeared light and SOFG-positive stained regions appeared dark. Images were analyzed using the threshold function with a black to red ratio of 1:3. The percentage of GAG coverage was then measured for each section.

Statistical analysis

Statistical analysis was performed using R (R Foundation for Statistical Computing, Vienna, Austria). A Wilcoxon rank sum test was used for all analyses (level of significance $\alpha = 0.05$). Three rabbits contributed to both contralateral and operated groups. To assess mechanical heterogeneity, the analysis unit was a knee and 3 independent observations were considered. Thus, within each group, ratios of anisotropy ($n = 3$), regional ($n = 3$) and site variations ($n = 3$) were each compared to 1. To assess the effect of OA on the global reduced modulus, the analysis unit was an animal and 3 independent observations were considered. Ratios between operated and contralateral mean reduced moduli of each animal ($n = 3$) were each compared to 1.

Results

Mechanical properties

For both groups, mean reduced moduli were obtained by averaging the eight local moduli per knee, corresponding to each site, region and direction. The average reduced modulus of operated menisci (1.1 ± 0.20 MPa) significantly decreased with OA ($P = 0.03$). It was about two times lower than in contralateral menisci (2.3 ± 0.69 MPa).

Effect of OA on the heterogeneity of meniscus mechanical properties

R_{ani}, R_{reg} and R_{site}, are presented in Table I, for both groups.

R_{ani} values were significantly ($P = 0.03$) higher than 1 in contralateral and operated menisci. Surprisingly, the ratios of the contralateral and operated menisci had closed mean values of 1.93 and 2.23, respectively. For both groups, the menisci were significantly more resistant in circumferential direction.

R_{reg} values were significantly lower than 1 ($P = 0.03$) in contralateral and operated menisci. The ratios were similar between contralateral and operated menisci, with mean values of 0.42 and 0.39, respectively. This result means that contralateral and operated menisci were significantly less resistant in the posterior region.

R_{site} was not significantly different ($P = 0.3$) from 1 in contralateral or operated menisci, with mean values of 1.21 and 1.07, respectively.

Table I
R_{ani} ratio between the moduli in circumferential and vertical directions ($n = 3$), R_{reg} ratio between the moduli in posterior and anterior regions ($n = 3$) and R_{site} ratio between the moduli in medial and lateral sites ($n = 3$), for contralateral and operated menisci. In each knee, R_{ani}, R_{reg} and R_{site} averaged the four dependent ratios, corresponding to the sites/regions, sites/directions and regions/directions, respectively. Results are presented as the mean ± standard deviation. *P* corresponds to ratio vs 1

Mean ratio	R_{ani}	R_{reg}	R_{site}
Contralateral	1.93 ± 0.64 ($P = 0.03$)	0.42 ± 0.23 ($P = 0.03$)	1.21 ± 0.51 ($P = 0.3$)
Operated	2.23 ± 0.16 ($P = 0.03$)	0.39 ± 0.13 ($P = 0.03$)	1.07 ± 0.77 ($P = 0.3$)

Chemical composition

Typical Raman spectra of contralateral and operated menisci are given in Fig. 3. The main collagen bands were proline ring (857 cm^{-1}), hydroxyproline ring (877 cm^{-1}), the vibrational modes of amide III structures (1220–1280 cm^{-1}), C–H bond bending mode (1447–1452 cm^{-1}) and vibrational modes of amide I structures (1600–1720 cm^{-1}). Raman spectral signature was not significantly modified at this stage of OA. Peaks assigned to hydroxyapatite (HA) (960 cm^{-1}) and calcium pyrophosphate dihydrate (CPPD) (1049 cm^{-1}) crystals were not identified in either contralateral or operated spectra, indicating the absence of mineralization[31].

Collagen microstructure

3D reconstructions of typical image stacks of tibial plane acquisitions are shown for contralateral (Fig. 4) and operated (Fig. 5) menisci. Contralateral menisci displayed well-organized, straight and compact collagen bundles along circumferential direction. This organization did not depend on the site (Fig. 4) or the region (data not shown). In contrast, operated menisci displayed less organized and less compact bundles where collagen was rather organized in wavy isolated fibers. These changes were observed in medial and lateral menisci (Fig. 5), in both regions (data not shown). Elastin fibers were not detected in any samples, as revealed by the absence of signal in its channel.

GAG content

Representative histological sections of contralateral and operated menisci are shown in Fig. 6. Contralateral menisci displayed weak red staining [Fig. 6(A)]. GAGs were mainly concentrated in the inner region. In operated menisci, the red-stained area expanded radially outwards [Fig. 6(B)]. GAG staining was especially more evident in the areas where the collagen fibers were not well aligned and displayed strong undulations [Fig. 6(C)–(D)]. Measurements of red coverage revealed that GAG content significantly increased with OA ($P = 0.03$), increasing from 11 ± 4.5 % in the contralateral group to 19.4 ± 7.6 % in the operated group [Fig. 6(E)].

Discussion

In the present study, the mechanical, chemical and microstructural properties of the menisci were compared in operated (ACLT) and contralateral rabbit knees through microindentation, RM and BCM. These non-destructive techniques were used on the same samples to provide complementary data of the tissue properties. The ACLT rabbit model of OA has been used previously to

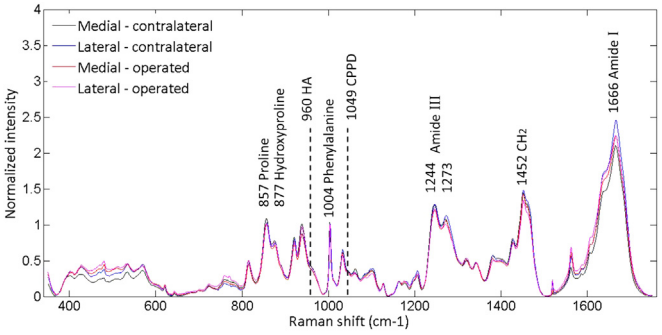

Fig. 3. Raman spectra of contralateral and operated menisci in medial and lateral sites. Presence of the main collagen bands. Absence of the crystal bands (HA, CPPD).

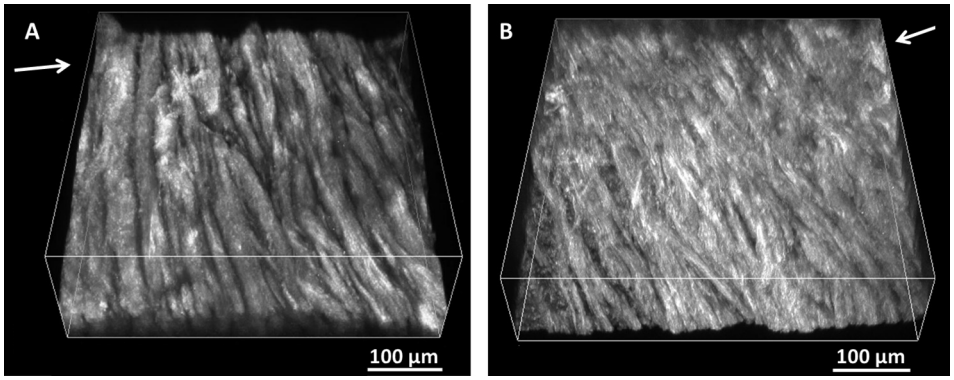

Fig. 4. Circumferential collagen fibers arrangement in A) medial and B) lateral contralateral menisci. The arrow indicates the radial direction, corresponding to the *x*-axis, and is oriented towards the center of the meniscus. Images' size: 509.12 µm × 509.12 µm × 150 µm.

determine the morphological, histological and chemical changes in menisci[16,32]. However, to date, no study has correlated these changes with mechanical alterations. This study demonstrates that this model of OA strongly affects the mechanical properties of the meniscus, which can be explained by microstructural modifications.

This study revealed an alteration of the mechanical properties of the menisci due to experimental OA. The reduced modulus was two times lower for operated menisci (1.1 ± 0.20 MPa) than contralateral (2.3 ± 0.69 MPa) menisci. Interestingly, the mean reduced modulus of contralateral menisci is of the same order of magnitude as those found for healthy menisci of bovine (1.2 MPa)[33], rabbit (1 MPa)[17], minipig (1.9 MPa)[34] and human (3.6–4 MPa)[35,36], using similar indentation tests. To our knowledge, it is the first time that mechanical properties of menisci are compared between operated and contralateral rabbit knees, using an ACLT model. The results obtained for the operated menisci are consistent with those obtained by Baro *et al.*[33] using a chemically induced model of OA on bovine menisci at an early stage, and those obtained by Fischenich *et al.*[17] using a mechanically induced model of OA in rabbits, where the ACL and both menisci were transected at a more advanced stage. They reported a decrease in Hertz moduli by 50% and 70%, respectively. On human menisci at end-stage OA, Katsuragawa *et al.*[8] observed the same trend on the aggregate modulus, which represents the stiffness of the tissue at equilibrium when all fluid flow has ceased. However, the results obtained for human tissues are controversial, as Kwok *et al.*[7] showed that Hertz modulus was two times higher at advanced stage OA compared to healthy menisci.

RM analyses revealed a conservation of the collagen secondary structure at this early stage of OA. This technique has already been used to characterize the structural alterations of collagen in OA cartilage[37] and synovial fluid[38], but questions remained regarding the menisci. As expected, the different peaks assigned to collagen were present in contralateral and operated menisci. No difference in their intensity was found between the two groups, whereas an increase in the amide I ratio[38] and the amide III ratio[37] were observed at the first stage of OA in synovial fluid and cartilage, respectively. These higher ratios correspond to the higher content of disordered collagen, which is an indicator of defective collagen[37].

RM also revealed an absence of mineralization in the meniscus at this stage of OA, even though calcification is common in the menisci of end-stage OA in human patients[10,11], and biomechanical properties are altered[11]. Indeed, Katsamenis *et al.*[31] found that CPPD crystallinities develop within the meniscal extracellular matrix and completely disrupt the collagen fibers, hindering the cohesion of the tissue. At this stage of OA in rabbits, the decrease in the mechanical properties of the menisci is not due to the formation of calcification.

BCM revealed an alteration of the collagen fiber architecture with OA. In contralateral menisci, the circumferential collagen fibers were straight, aligned and organized in compact bundles, providing the menisci with high mechanical strength[39]. It is consistent with previous studies on healthy menisci from

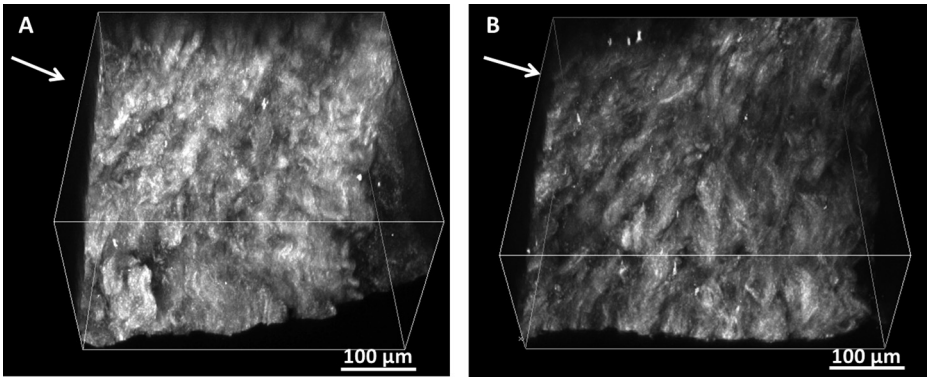

Fig. 5. Circumferential collagen fibers arrangement in A) medial and B) lateral operated menisci. The arrow indicates the radial direction, corresponding to the *x*-axis, and is oriented towards the center of the meniscus. Images' size: 509.12 µm × 509.12 µm × 200 µm.

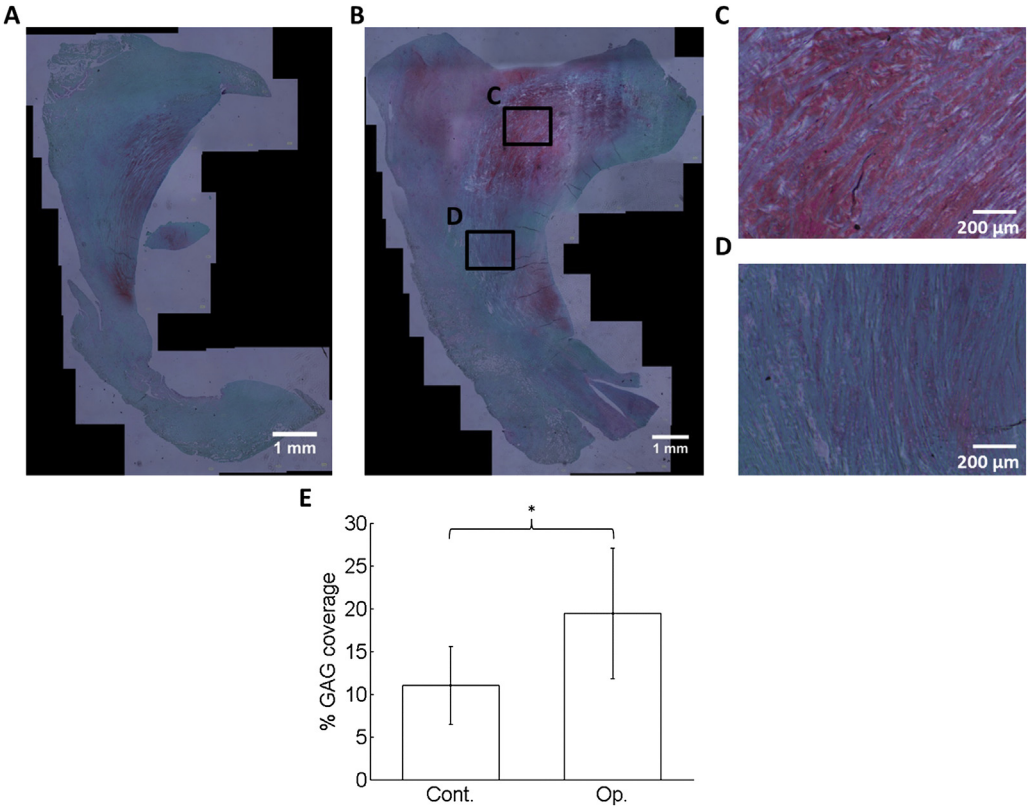

Fig. 6. Representative images of SOFG staining in A) contralateral (Cont.) and B) operated (Op.) menisci. The sections correspond to the same animal. Boxes indicate the location of the following detail images; C) (C in B) close-up of an intensely stained area. Collagen fibers were highly undulated and not well aligned; D) (D in B) close-up of a weakly stained area. Collagen fibers were straighter and less unorganized; E) mean percent area of GAG coverage and SD bars ($n = 3$). * corresponds to $P < 0.05$.

human[8–10,25,39,40] and rabbit samples[40,41]. In operated menisci, these bundles were less compact, which was also observed in histological studies on human OA menisci[8–10]. Moreover, undulation of the collagen fibers indicated that they were not under tension anymore. These changes resulted in a loss of mechanical resistance of the fibers, which explains the decrease in the reduced modulus of the menisci. However, the fibers in operated menisci were still aligned and oriented in the circumferential direction. Consequently, the anisotropic behavior observed in contralateral menisci, which has been highlighted previously using tensile tests[42–44], was also observed in operated menisci. In both groups, the reduced modulus was two times higher in the circumferential direction than in the vertical direction. This observation suggests that the disorganized fibers continue to resist hoop stresses.

Histological analyses revealed an increase in GAG content after induction of OA. This is in agreement with previous studies on human OA menisci[7,9,10,45] and rabbit using an ACLT model[16]. Although GAGs are highly responsible for the mechanical resistance of cartilage in compression[46], their role in the mechanical resistance of the meniscus is not fully understood. Recently, Fischenich *et al.*[17] and Kwok *et al.*[7] found a positive correlation between GAG content and instantaneous modulus in rabbit and human OA menisci, respectively. However, Sanchez-Adams *et al.*[20] showed that GAG depletion in the outer region of bovine menisci did not change the instantaneous modulus. Similarly, Son *et al.*[19] did not find any significant correlation between GAG content and equilibrium compressive modulus in human OA menisci. Our results support these two later studies because the reduced modulus decreased while GAG content increased.

This finding, together with the disorganization of the collagen framework, is consistent with the structure-function relationships of the meniscus proposed by Vanderploeg *et al.*[18]. They suggest that compressive forces that develop in the inner zones are resisted by GAGs, while circumferential tensile forces in the outer zones are resisted by collagen fibers. The increase in GAG content can then be seen as a response to the collagen degradation and an attempt to compensate for the loss of mechanical resistance[10]. Indeed, GAGs were concentrated in the areas where collagen fibers were undulated and less organized, corresponding to areas of low tensile properties. This is consistent with the study by Herwig *et al.*[45], which reported that in human patients with meniscal lesions, GAG content increased with the severity of meniscal degradation.

In this study, the two analyzed regions of medial and lateral menisci were mechanically impacted by OA. Indeed, we showed that OA drastically decreased the mean reduced modulus of the menisci. In addition, the ratio between anterior and posterior reduced moduli (R_{reg}) was similar between contralateral and operated groups, as well as with the ratio between medial and lateral reduced moduli (R_{site}). This result clearly shows that OA induced by ACLT has a global effect over the menisci. Interestingly, the anterior region was about three times stiffer than the posterior region. This heterogeneity is consistent with other studies on human[33,47] and rabbit[48] healthy menisci. These results on the mechanical properties are not surprising since the collagen framework was disorganized in both regions of medial and lateral menisci. However, in the literature, the medial meniscus was generally the most affected macroscopically following an ACLT, especially in the posterior region[16]. Nevertheless, more rabbits would be necessary to find out if mechanical alterations are significantly more severe in the posterior medial meniscus.

In conclusion, this study demonstrates that a degradation of the collagen framework occurs in the whole menisci following ACLT in

this rabbit model. This damage leads to a loss of mechanical resistance of the menisci. The significant increase in GAG content within the damaged areas was attributed to an attempt to compensate for the loss of mechanical resistance. Altogether, these results provide a better understanding of the disease process affecting the meniscus. An important consideration of this study is the stage of OA. All of the mechanical and matrix alterations occur during the early phases of OA development following ACLT. This puts forward the necessity for early diagnosis and treatment to prevent, or at least slow down, its progression. Future studies will aim to evaluate the efficacy on the meniscus of intra-articular viscosupplementation therapy formulation.

Contributions

All authors have made substantial contributions to this study.

Aurélie Levillain contributed to study design, data collection, analysis and interpretation of the data, drafting of the manuscript and final approval of the article.

Caroline Boulocher contributed to study design, interpretation of the data, drafting and critical revision of the article for important intellectual content and final approval of the article.

Sema Kaderli provided the study materials, contributed to critical revision of the article for important intellectual content and final approval of the article.

Didier Hannouche, Eric Viguier, Thierry Hoc and Hélène Magoariec contributed to study design, critical revision of the article for important intellectual content and final approval of the article.

Role of the funding source

None.

Competing interests

None.

Acknowledgments

The authors wish to thank biovivo from the Claude Bourgelat Institute (IClB), Lyon, France, for the animal care and logistical support; Dorothée Virieux-Watrelot, Guillaume Fargier and Catherine Bosser for their technical support. We would also like to thank the IVTV ANR-10-EQPX-06-01 for their financial support.

Supplementary data

Supplementary data related to this article can be found at http://dx.doi.org/10.1016/j.joca.2015.02.022.

References

1. Makris EA, Hadidi P, Athanasiou KA. The knee meniscus: structure-function, pathophysiology, current repair techniques, and prospects for regeneration. Biomaterials 2011;32:7411–31.
2. Hunter DJ, Zhang YQ, Niu JB, Tu X, Amin S, Clancy M, *et al*. The association of meniscal pathologic changes with cartilage loss in symptomatic knee osteoarthritis. Arthritis Rheum 2006;54:795–801.
3. Iijima H, Aoyama T, Ito A, Tajino J, Nagai M, Zhang X, *et al*. Destabilization of the medial meniscus leads to subchondral bone defects and site-specific cartilage degeneration in an experimental rat model. Osteoarthritis Cartilage 2014;22:1036–43.
4. Zarins Z, Bolbos R, Pialat J, Link T, Li X, Souza R, *et al*. Cartilage and meniscus assessment using T1rho and T2 measurements in healthy subjects and patients with osteoarthritis. Osteoarthritis Cartilage 2010;18:1408–16.
5. Berthiaume M-J, Raynauld J-P, Martel-Pelletier J, Labonte F, Beaudoin G, Bloch DA, *et al*. Meniscal tear and extrusion are strongly associated with progression of symptomatic knee osteoarthritis as assessed by quantitative magnetic resonance imaging. Ann Rheumatic Dis 2005;64:556–63.
6. Lange AK, Singh MAF, Smith RM, Foroughi N, Baker MK, Shnier R, *et al*. Degenerative meniscus tears and mobility impairment in women with knee osteoarthritis. Osteoarthritis Cartilage 2007;15:701–8.
7. Kwok J, Grogan S, Meckes B, Arce F, Lal R, D'Lima D. Atomic force microscopy reveals age-dependent changes in nanomechanical properties of the extracellular matrix of native human menisci: implications for joint degeneration and osteoarthritis. Nanomedicine 2014;10(8):1777–85.
8. Katsuragawa Y, Saitoh K, Tanaka N, Wake M, Ikeda Y, Furukawa H, *et al*. Changes of human menisci in osteoarthritic knee joints. Osteoarthritis Cartilage 2010;18:1133–43.
9. Sun Y, Mauerhan DR, Kneisl JS, Norton HJ, Zinchenko N. Histological examination of collagen and proteoglycan changes in osteoarthritic menisci. Open Rheumatology J 2012;6:24–32.
10. Pauli C, Grogan S, Patil S, Otsuki S, Hasegawa A, Koziol J, *et al*. Macroscopic and histopathologic analysis of human knee menisci in aging and osteoarthritis. Osteoarthritis Cartilage 2011;19:1132–41.
11. Sun Y, Mauerhan DR, Honeycutt PR, Kneisl JS, Norton HJ, Zinchenko N. Calcium deposition in osteoarthritic meniscus and meniscal cell culture. Arthritis Res Ther 2010;12(56).
12. Madry H, Luyten FP, Facchini A. Biological aspects of early osteoarthritis. Knee Surg Sports Traumatol Arthrosc 2012;20:407–22.
13. Mäkelä J, Rezaeian Z, Mikkonen S, Madden R, Han S-K, Jurvelin J, *et al*. Site-dependent changes in structure and function of lapine articular cartilage 4 weeks after anterior cruciate ligament transection. Osteoarthritis Cartilage 2014;22:869–78.
14. Turunen S, Han S-K, Herzog W, Korhonen R. Cell deformation behavior in mechanically loaded rabbit articular cartilage 4 weeks after anterior cruciate ligament transection. Osteoarthritis Cartilage 2013;21:505–13.
15. Sonoda M, Harwood FL, Amiel ME, Moriya H, Amiel D. The effects of hyaluronan on the meniscus in the anterior cruciate ligament-deficient knee. J Orthop Sci 2000;5:157–64.
16. Hellio Le Graverand M-P, Vignon E, Otterness IG, Hart DA. Early changes in lapine menisci during osteoarthritis development: part I: cellular and matrix alterations. Osteoarthritis Cartilage 2001;9:56–64.
17. Fischenich K, Coatney G, Haverkamp J, Button K, DeCamp C, Haut R, *et al*. Evaluation of meniscal mechanics and proteoglycan content in a modified anterior cruciate ligament transection model. J Biomechanical Eng 2014;136(7).
18. Vanderploeg EJ, Wilson CG, Imler SM, Ling CH-Y, Levenston ME. Regional variations in the distribution and colocalization of extracellular matrix proteins in the juvenile bovine meniscus. J Anat 2012;221:174–86.
19. Son M, Goodman S, Chen W, Hargreaves B, Gold G, Levenston M. Regional variation in T1 r and T2 times in osteoarthritic human menisci: correlation with mechanical properties and matrix composition. Osteoarthr Cartil 2013;21:796–805.

20. Sanchez-Adams J, Willard VP, Athanasiou KA. Regional variation in the mechanical role of knee meniscus glycosaminoglycans. J Appl Phys 2011;111:1590–6.
21. Vignon E, Bejui J, Mathieu P, Hartmann J, Ville G, Evreux J, *et al*. Histological cartilage changes in a rabbit model of osteoarthritis. J Rheumatology 1987;14:104–6.
22. Yoshioka M, Coutts R, Amiel D, Hacker S. Characterization of a model of osteoarthritis in the rabbit knee. Osteoarthritis Cartilage 1996;4:87–98.
23. Nisbet HO, Ozak A, Yardimci C, Nisbet C, Yarim M, Bayrak I, *et al*. Evaluation of bee venom and hyaluronic acid in the intra-articular treatment of osteoarthritis in an experimental rabbit model. Res Veterinary Sci 2010:488–93.
24. Pailler-Mattei C, Laquièze L, Debret R, Tupin S, Aimond G, Sommer P, *et al*. Rheological behaviour of reconstructed skin. J Mech Behav Biomed Mater 2014;37:251–63.
25. Petersen W, Tillmann B. Collagenous fibril texture of the human knee joint menisci. Anat Embryol 1998;197:317–24.
26. Oliver W, Pharr G. An improved technique for determining hardness and elastic modulus using load displacement sensing indentation experiments. J Mater Res 1992;7(6):1564–83.
27. Morris MD, Mandair GS. Raman assessment of bone quality. Clin Orthop Relat Res 2011;469(8):2160–9.
28. Kuzuhara A. Analysis of structural changes in bleached keratin fibers (black and white human hair) using Raman spectroscopy. Biopolymers 2006;81(16):506–14.
29. Rasband WS. ImageJ, U. S. National Institutes of Health. Maryland, USA: Bethesda, http://imagej.nih.gov/ij/; 1997–2014.
30. Killian ML, Lepinski NM, Haut RC, Haut Donahue TL. Regional and zonal histo-morphological characteristics of the lapine menisci. Anat Rec 2010;293:1991–2000.
31. Katsamenis OL, Karoutsos V, Kontostanos K, Panagiotopoulos EC, Papadaki H, Bouropoulos N. Microstructural characterization of CPPD and hydroxyapatite crystal depositions on human menisci. Cryst Res Technol 2012;47(11):1201–9.
32. Hellio Le Graverand M-P, Vignon E, Otterness IG, Hart DA. Early changes in lapine menisci during osteoarthritis development part II: molecular alterations. Osteoarthr Cartil 2001;9:65–72.
33. Baro VJ, Bonnevie ED, Lai X, Price C, Burris DL, Wang L. Functional characterization of normal and degraded bovine meniscus: rate-dependent indentation and friction studies. Bone 2012;51:232–40.
34. Li X, An YH, Wu Y-D, Song YC, Chao YJ, Chien C-H. Microindentation test for assessing the mechanical properties of cartilaginous tissue. J Biomed Mater Res Part B: Appl Biomaterials 2007;80(1):25–31.
35. Moyer JT, Priest R, Bouman T, Abraham AC, Haut Donahue TL. Indentation properties and glycosaminoglycan content of human menisci in the deep zone. Acta Biomater 2013;9(5):6624–9.
36. Moyer JT, Abraham AC, Haut Donahue TL. Nanoindentation of human meniscal surfaces. J Biomechanics 2012;45:2230–5.
37. Takahashi Y, Sugano N, Takao M, Sakai T, Nishii T, Pezzotti G. Raman spectroscopy investigation of load-assisted microstructural alterations in human knee cartilage: preliminary study into diagnostic potential for osteoarthritis. J Mech Behav Biomed Mater 2014;31:77–85.
38. Esmonde-White KA, Mandair GS, Raaii F, Jacobson JA, Miller BS, Urquhart AG, *et al*. Raman spectroscopy of synovial fluid as a tool for diagnosing osteoarthritis. J Biomed Opt 2009;14(3).
39. Rattner JB, Matyas JR, Barclay L, Holowaychuk S, Sciore P, Lo IKY, *et al*. New understanding of the complex structure of knee menisci: implications for injury risk and repair potential for athletes. Scandinave J Med Sci sports 2011;21:543–53.
40. Chevrier A, Nelea M, Hurtig MB, Hoemann CD, Buschmann MD. Meniscus structure in human, sheep, and rabbit for animal models of meniscus repair. J Orthop Res 2009;27(1197):203.
41. Ghadially FN, Thomas I, Yong N, Lalonde J-MA. Ultrastructure of rabbit semilunar cartilages. J Anat 1978;125(3):499–517.
42. Bullough PG, Munuera L, Murphy J, Weinstein AM. The strength of the menisci of the knee as it relates to their fine structure. J Bone Joint Surg 1970;53(3):564–70.
43. Tissakht M, Ahmed AM. Tensile stress-strain characteristic of the human meniscal material. J Biomechanics 1995;28(4):411–22.
44. Goertzen D, Budney D, Cinats J. Methodology and apparatus to determine material properties of the knee joint meniscus. Med Eng Phys 1997;19(5):412–9.
45. Herwig J, Egner E, Buddecke E. Chemical changes of human knee joint menisci in various stages of degeneration. Ann Rheum Dis 1984;43:635–40.
46. Mansour JM. Biomechanics of cartilage. In: Kinesiology: the Mechanics and Pathomechanics of Human Movement. Philadelphia: Lippincott Williams and Wilkins; 2003:66–79.
47. Chia HN, Hull ML. Compressive moduli of the human medial meniscus in the axial and radial directions at equilibrium and at a physiological strain rate. J Orthop Res 2008;26(7):951–6.
48. Sweigart M, Zhu CF, Burt DM, Deholl PD, Agrawal CM, Clanton TO, *et al*. Intraspecies end interspecies comparison of the compressive properties of the medial meniscus. J Biomed Eng 2004;32(11):1569–79.